Polymer Journal (2012) 44, 1179–1190

www.nature.com/pj

INVITED REVIEW

The synthesis of copolymers, blends and composites based on poly(butylene succinate)

Sung Yeon Hwang[1], Eui Sang Yoo[2] and Seung Soon Im[1]

Poly(butylene succinate) (PBS) is one of the most available environmentally degradable polymers used in industrial applications. Biodegradable polyesters including PBS have low thermal stability, poor mechanical properties and slow crystallization rates. For this reason, many researchers have investigated PBS composites, especially nanocomposites with functional inorganic materials, to identify other advanced properties. We used two inorganic materials to investigate how nanoparticles could be dispersed in a PBS matrix and to identify the properties that could be advanced by fabricating well-dispersed PBS nanocomposites. Clay and zeolite were used for the nano components because they are well known and widely used inorganic materials in polymer-inorganic nanocomposites. The most challenging problem when fabricating the clay–polymer nanocomposite has been how to separate the clay layers in the composite to overcome the very strong cohesive energies between the clay layers. Numerous studies have introduced modifiers into silicate layers to increase the basal space and facilitate easier polymer chain incorporation. We introduce a urethane group on a clay surface to develop physically enhanced PBS/montmorillonite (MMT) nanocomposites. A series of PBS-based ionomers are synthesized by two-step polycondensation. This study focuses on the effect of the ionic group on dynamic mechanical properties, melt rheology, crystallization behavior and enzymatic hydrolysis.
Polymer Journal (2012) **44,** 1179–1190; doi:10.1038/pj.2012.157; published online 19 September 2012

Keywords: biodegradable polymer; clay; enzymatic hydrolysis; ionomer; nanocomposites; TS-1 zeolite

INTRODUCTION

There has been considerable interest in aliphatic biodegradable polyesters over the last decade because of increased concerns about environmental conservation.[1–9] Among aliphatic biodegradable polyesters, poly(butylene succinate) (PBS) is considered to be a promising material in many fields because it has excellent biodegradability, melt processibility and chemical resistance. However, PBS has limited applications because of its poor thermal stability and mechanical properties.

PBS/inorganic nanocomposites have been proposed to overcome these drawbacks, and are being developed as the next generation of biodegradable materials. Numerous studies of clay-based biodegradable polymer nanocomposites have focused on changes in preparation methods and morphological properties, as well as the enhancement of mechanical and thermal properties.[10,11] Ray *et al.*[10] investigated the degree of exfoliation of PBS/clay nanocomposites with various clay types and demonstrated control of the flocculation of dispersed silicate layers in PBS/clay nanocomposites. The achievement of a fine dispersion of the nanofiller in a polymer matrix is a key problem when attempting to produce biodegradable polymer/clay nanocomposites. As noted above, homogeneous clay dispersions in biodegradable polymer matrix are difficult to achieve because of the strong tendency of clay particles to agglomerate. In previous studies, biodegradable polymer nanocomposites with fully dispersed clay were obtained only when the following factors were considered:

1. The d-spacing between layered silicates: increases in the d-spacing made it easier to penetrate polymer chains into layered silicates.
2. Affinity between layered silicate and biodegradable polymers: increases in the hydrophobicity of layered silicate were beneficial for clay–polymer affinity.
3. Miscibility between modifiers and biodegradable polymers: similar solubility parameters between organic modifier and matrix polymer were beneficial for modifier–polymer miscibility.

Copolymerization is important for improving the mechanical properties of PBS. However, several factors affect the physicochemical properties of PBS, such as melting point depression due to imperfect lateral packing in the lamellae or isomorphism.[12–15] In order to overcome these shortcomings, the ionomer concept has been employed in the field of PBS.[16–22] An ionomer is defined as an ion-containing polymer with a small amount (usually up to 10–15 mol%) of ionic groups along the backbone chains or as pendant groups. Ionomers have been extensively studied because they exhibit significant changes in their physical properties owing to the formation of ionic aggregates such as enhanced mechanical properties, high melt viscosity and increased thermal properties.[23–25]

Many previous studies have explored co-polyester-based ionomers and nanocomposites with inorganic particles based on the PBS matrix.[26–39] These papers mainly focused on the enhancement

[1]Department of Fiber and Polymer Enginering, College of Engineering, Hanyang University, Seoul, Korea and [2]Convergent Technology R&D Division, Department of Textile Convergence of Biotechnology & Nanotechnology, Korea Institute of Industrial Technology, Ansan City, Korea
Correspondence: Professor SS Im, Department of Fiber and Polymer Engineering, College of Engineering, Hanyang University, 17 Haengdang-dong, Seongdong-gu, Seoul 133-791, Korea.
E-mail: imss007@hanyang.ac.kr
Received 22 May 2012; accepted 29 June 2012; published online 19 September 2012

of physical properties as well as the control of biodegradability, because applications for PBS have increased over time, including uses in medicine, pharmacy, agriculture and packaging.

This review summarizes our recent studies of the characteristics of nanocomposites and ionomer-based PBS produced for use as a biodegradable polyester.

PBS/INORGANIC FILLER NANOCOMPOSITES

We used two inorganic materials to investigate how nanoparticles could be dispersed in a PBS matrix and to identify the kinds of properties that could be advanced by producing well-dispersed PBS nanocomposites. Clay and zeolite were used as the nano components because they are well-known and widely used inorganic materials in polymer–inorganic nanocomposites.

PBS/modified clay nanocomposites

The most challenging problem when fabricating the clay–polymer nanocomposite has been how to separate the clay layers in the composite to overcome the strong cohesive energy between the layers. Many previous studies focused on introducing modifiers into silicate layers to increase the basal space for easier polymer chain incorporation. In this study, we started from a different point, by introducing covalent bonds between silica layers and the modifier using a diisocyanate coupling agent such as 1,6-diisocyanatohexane (HDI). Then, we introduced a urethane group on the clay surface to develop physically enhanced PBS/montmorillonite (MMT) nanocomposites.

Figure 1 shows a schematic diagram of the procedure and the modified clay surface for making PBS/MMT nanocomposites. PBS/MMT nanocomposites were prepared by *in situ* polymerization consisting of direct esterification and polycondensation.

Clay surface urethane modification is intended to increase basal spacing, to make it easier for polymer chains to penetrate into clay layers. X-ray diffraction (XRD) allows the exact evaluation of basal spacing. Figure 2 presents wide-angle X-ray diffraction (WAXD) profiles indicating (A) the basal spacing of clays and (B) the intercalation spacing of prepared nanocomposite samples. The notations 10A and 30B indicate 10A-MMT and 30B-MMT, respectively. Here, 10A and 30B are alkyl modifiers containing MMT with modifier concentrations of 125 and 95 meq/100 g clay, respectively. Urethane-modified clay is designated as 30BM. PBS/MMT nanocomposites are denoted as clay-type contents such as 30BM10. In Figure 2A, modified clay (30BM) shows the widest basal spacing. This increased basal spacing reduced the physical affinities between silicate layers,

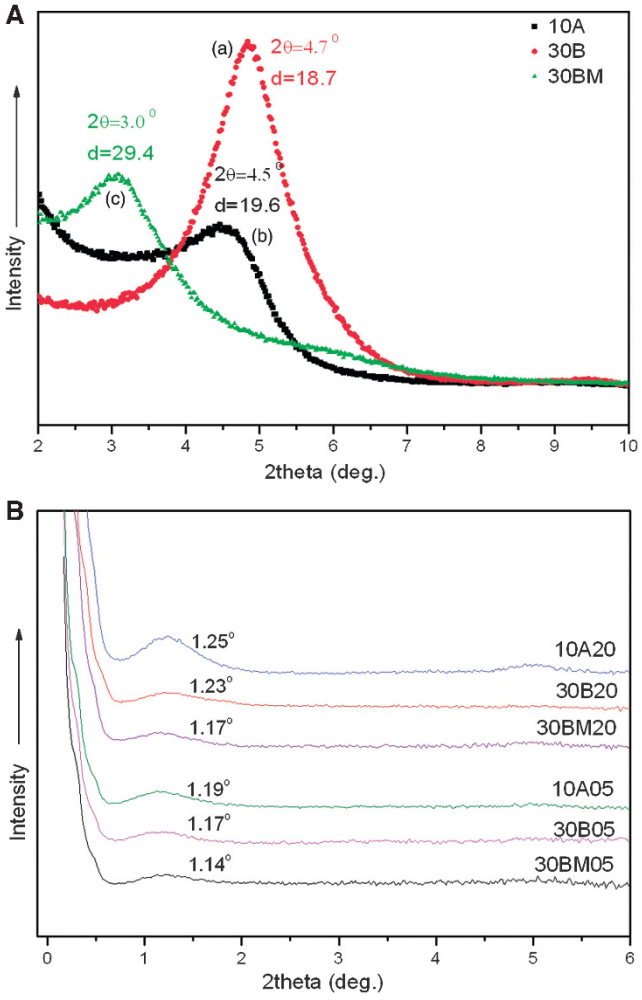

Figure 2 Wide-angle X-ray diffraction (WAXD) profiles (**A**) of various clays: (a) 10A, (b) 30B and (c) 30BM; WAXD profiles (**B**) of nanocomposites.

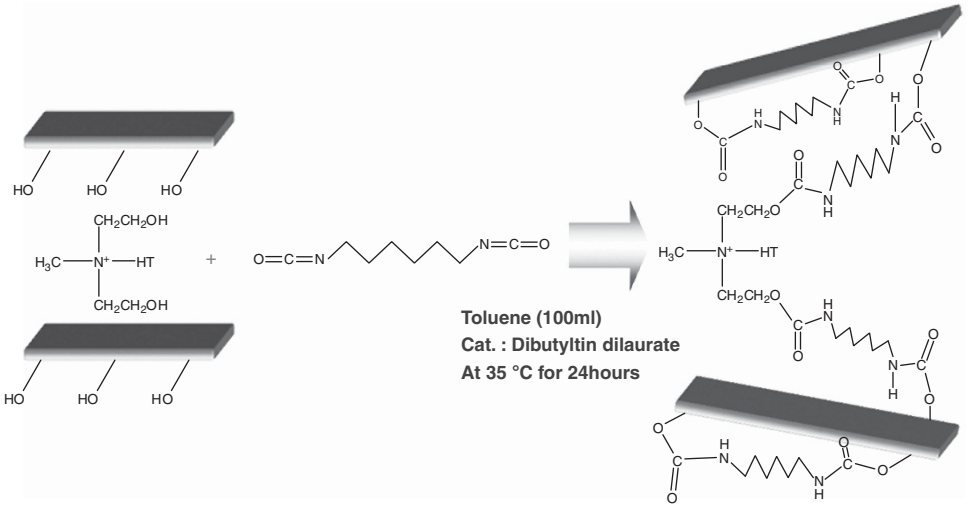

Figure 1 The formation of covalent bonds between silanol groups in montmorillonite (MMT) or silanol groups and the hydroxyl group of organic modifiers by 1,6-diisocyanatohexane (HDI) for clay surface treatment. A full color version of this figure is available at *Polymer Journal* online.

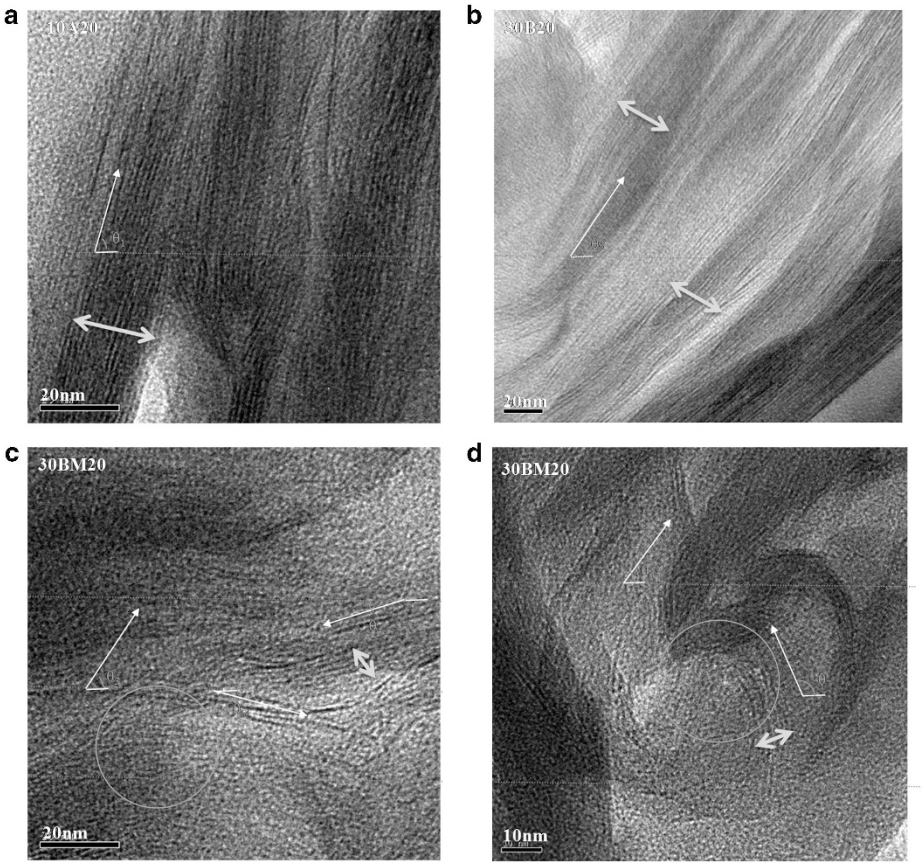

Figure 3 Transmission electron microscopy (TEM) micrographs of nanocomposites composed of (**a**) 10A20, (**b**) 30B20, (**c**) 30BM20 and (**d**) 30BM20 (at a 10-nm resolution). A full color version of this figure is available at *Polymer Journal* online.

making it easier for the PBS chains to penetrate into silicate layers and to form an exfoliation structure. Figure 2B shows that this assumption is correct. When the same amount of clay is introduced, the modified clay with urethane groups inside the clay layers more easily accept PBS molecular chains, resulting in a low diffraction angle of the *d*(001) plane of the dispersed silicate layers in the PBS matrix. This may have occurred because the surface urethane modification in 30BM decreased the physical attraction between silicate–silicate and allowed the PBS matrix to permeate into the silicate layers; this favorable effect resulted in easier exfoliation.[40]

Transmission electron microscopy images provide further evidence to confirm disordered clay dispersion. As shown in Figures 3a and b (10A20 and 30B20, respectively), clay sheets were uniformly oriented with complete layer stacks containing an average of 14 and 12 silicate sheets per bundle, respectively. In contrast, Figures 3c and d (30BM20) reveal significantly smaller bundles composed of only 3–4 randomly oriented silicate sheets. In this figure, $\theta_{1\sim7}$ was introduced to explain the degree of orientation of the silicate sheets. In the areas indicated by red circles, an omni-directional angle of dispersed clay layer can be seen, indicating largely exfoliated clay sheets in the PBS matrix.

Further, we conclusively demonstrated that urethane-modified MMT nanocomposites yield superior clay exfoliation because the alkyl chains of a coupling agent are effectively introduced by covalent bonding between the silica layers and modifiers. In the PBS/modified MMT nanocomposite, better affinity between the PBS molecules and the surface of modified MMT allowed for better incorporation of PBS molecules into silicate layers. These results contributed to the improved physical properties of PBS/MMT nanocomposites. Further, 30BM nanocomposites showed considerably improved tensile strengths and Young's moduli as well as elongation at breaks compared with 10A and 30B nanocomposites. When nanoparticles are introduced, both the tensile strength and elongation at breaks decreased drastically with increasing clay content because of the increased stiffness and formation of microvoids around clay particles during tensile testing. We observed this phenomenon in 10A and 30B nanocomposites; however, 30BM samples with high clay content were able to maintain all physical properties without deviation. This result indicates that surface modification of clay diminishes microvoids,[41] resulting in a fine dispersion of clay in the PBS matrix, and that adding urethane groups to a clay surface increased the physical affinity between the clay and PBS matrix; these are the two most significant driving forces for exfoliation nanostructure. This explanation was verified as shown in Figure 4, which shows scanning electron microscopy (SEM) images of the fracture surface of the PBS/MMT nanocomposite after the tensile test.

Our findings indicate that several types of interactions should be considered to improve the mechanical properties of MMT nanocomposites: silicate–silicate interaction, silicate–polymer interaction and modifier–polymer interaction. First, modifiers can produce larger gaps between silicates, which are known to improve the ease of exfoliation by reducing the silicate–silicate attraction. Second, the

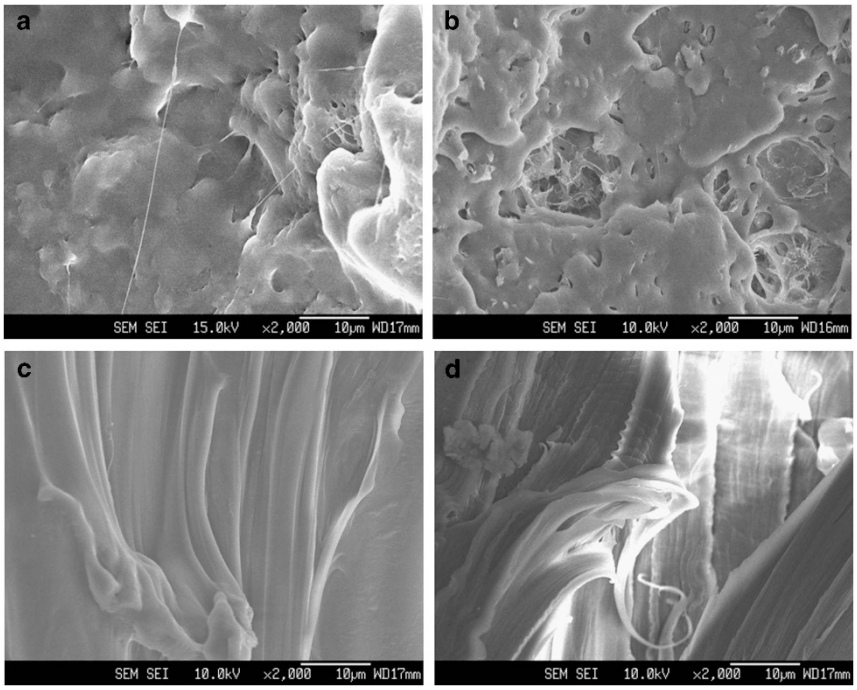

Figure 4 SEM micrographs of nanocomposites composed of (**a**) poly(butylene succinate) (PBS), (**b**) 10A05, (**c**) 30B05 and (**d**) 30BM05.

increasing density of alkyl modifier tails affects exfoliated nanocomposites because excess organic alkyl modifier tails can interfere with the favorable affinity between the silicate surface and PBS matrix.[40,41] 30BM had a wider basal spacing than 10A and 30B, and the urethane group introduced to the clay surface also improved the contact between the silicate–PBS matrix. The urethane surface modification of 30BM ensures appropriate preconditions, such as silicate–silicate interactions and silicate–polymer interaction, to allow for exfoliation.

The improved affinity between nanoparticles and the polymer matrix, as well as the improved dispersion of particles, may affect the crystallization behavior of a polymer nanocomposite. Crystallization behavior is one of the most important factors for polymer processing. Therefore, we investigated the nucleation effect of clay in PBS/urethane-modified MMT nanocomposites in the context of clay dispersion and the effectiveness of the urethane group using isothermal crystallization and by determining the activation energy for crystallization.

The Avrami equation was used for analyzing the crystallization kinetics of 30B20 and 30BM20. The 30B20 sample is a PBS/MMT(30B modifier-containing) nanocomposite without urethane modification, and 30BM20 was subjected to urethane modification. The crystallization rate of 30B20 was the greatest among all of the samples at the same isothermal temperature, indicating that the 30B clay can act as a nucleating agent to significantly increase the crystallization rate of PBS, whereas the crystallization rate of the 30BM20 was similar to that of homoPBS.

The isothermal crystallization rate of polymer nanocomposites increases with the addition of silicate layers.[42,43] In the clay composite, when clay contains an alkyl modifier, metallic groups are precluded by excess alkyl modifiers and have important roles in nucleation. The surface urethane modification for 30BM may cause PBS molecules to contact the metallic group and reduce the activity of the metallic group for nucleation, although the surface urethane modification led to partially exfoliated states of 30BM20. As a consequence, the crystallization rate of 30BM20 is similar to that of PBS. Urethane-modified clay nanocomposites showed spherulite growth because of heterogeneous nucleation similar to pure PBS or alkyl modifier-containing clay nanocomposites (30BM). Avrami exponent values of all the samples were in the range from 2.3 to 3.2. Crystallization activation energy was calculated using the Avrami kinetic parameter under the hypothesis that the crystallization process of bulk PBS was thermally activated. The clay in the PBS nanocomposite can increase the probability of nucleation, but also restrain the PBS molecules from moving for crystallization. This hypothesis was supported by the finding that the activation energy for the crystallization of a PBS/clay nanocomposite was higher than that of homoPBS ($-165\,J\,mol^{-1}$). The activation energy for crystallization of urethane-modified clay ($-171\,J\,mol^{-1}$) was lower than that of unmodified clay ($-206\,J\,mol^{-1}$), indicating that the introduction of urethane functional groups alleviates the restraint of PBS molecule movements against clay layers during crystallization by increasing the affinity between PBS molecules and clay layers with urethane groups.

Urethane group moieties in the PBS nanocomposite were supposed to increase the hydrophilicity of the surface compared with the unmodified clay composite (Figure 5). When only alkyl modifier was introduced into the clay (30B sample), the clay was revealed to be hydrophobic because of the long alkyl chains of the modifier, even though there were hydroxyl groups on the clay surface. This is why the 30B20 sample showed such a high contact angle compared with the homoPBS- or urethane-modified clay PBS composite. As discussed above, urethane groups may increase the affinity of PBS molecules to clay layers. In Figure 4, the SEM image shows that the microvoids, that were observed in the clay composite without urethane modification disappeared in the urethane-modified clay composite. Therefore, in this type of composite, clays may be well

covered with PBS molecules, and the surface of the composite may have the same hydrophilicity as homoPBS itself. However, the wetting rate increased in the urethane-modified clay composite because of the urethane group.

PBS/TS-1 zeolite hybrid composites

Clay is one of the most widely used inorganic nanoparticles for polymer composites. Clay has a layer structure, and most relevant research describes how to separate or exfoliate each layer to be dispersed in a polymer matrix. Zeolites are another type of inorganic nanoparticle that are widely used in many applications, including polymer composites. Zeolites, defined as highly ordered microporous materials, are used as heterogeneous catalysts in many reactions, such as aromatization, cracking, esterification, alkylation and methanol conversions. They are also used in petroleum refining as drying agents, ion exchangers, animal food additives, nuclear effluent treatment and membranes in numerous industrial fields.[44–46] Micropore size or structure is so important in zeolite functions that many researchers have tried to synthesize new ordered microporous materials.[47–49]

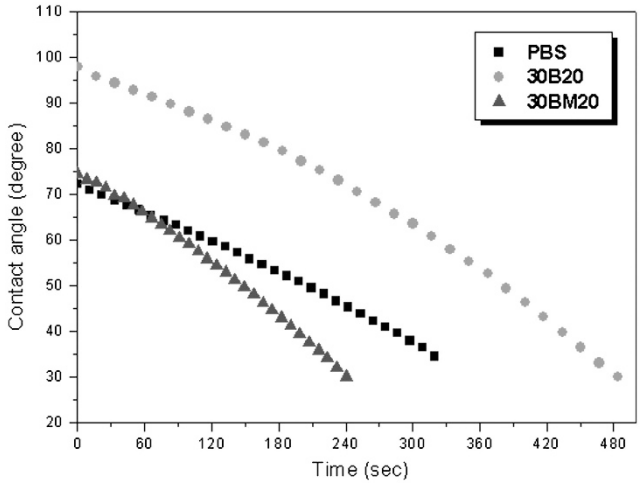

Figure 5 Variance in contact angle with increasing time. A full color version of this figure is available at *Polymer Journal* online.

We used titanium silicate-1 (TS-1) zeolite to produce PBS/zeolite nanocomposites, as it is one of the zeolite types with strong catalytic activity. We hypothesized that TS-1 zeolite could act as a catalyst during the esterification reaction in PBS synthesis. In addition to that, TS-1 has the advantage of having a high coordination ability of Ti^{4+} ions with the hydrophobic silicate framework. In particular, the adsorption of water molecules in the pores is closely associated with the surface structure, stability and activity of Ti sites in TS-1.[50–52] Figure 6 shows the pore size distribution and N_2 adsorption/desorption isotherms of TS-1 zeolite with SEM images.

The water uptake characteristics of TS-1 may affect the mechanical properties, hydrolytic degradability and melt processibility of PBS/TS-1 nanocomposites. We investigated water volatilization during melt processing of the nanocomposite. In Figure 7, absolute evidence for water volatilization of the nanocomposite was observed. The intensity of the water characteristic peak gradually increased with increasing temperature because of the release of water molecules from TS-1 zeolite pores by thermal energy.

These water molecule adsorption/desorption characteristics of the TS-1 zeolite in a PBS matrix affected the rheological properties in the melt state (150 °C), as shown in Figure 7c. HomoPBS showed a Newtonian plateau at low-shear-rate regions and shear thinning was observed for higher shear rates. The shear viscosity of PBS/TS-1 nanocomposite was higher than that of homoPBS, and exhibited shear thinning from the initial stage of the shear rate. We concluded

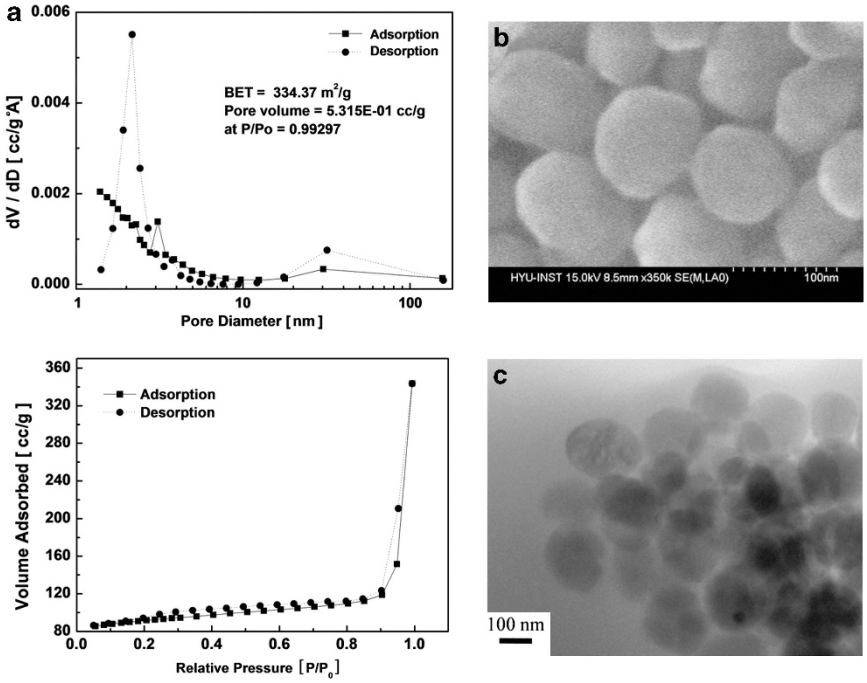

Figure 6 (**a**) Pore size distribution curves and N_2 adsorption/desorption isotherms of titanium silicate-1 (TS-1) zeolite, (**b**) SEM image of TS-1 zeolite at high magnification (× 350k) and (**c**) transmission electron microscopy (TEM) image of TS20.

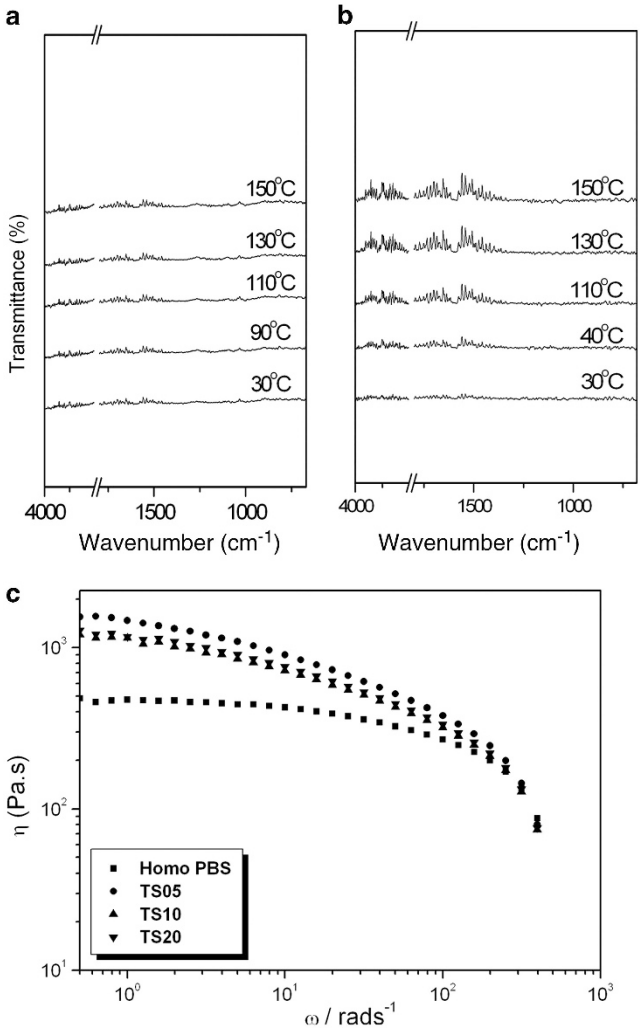

Figure 7 Thermogravimetric analysis coupled with infrared spectroscopy (TG-IR) spectra of volatilized water in (**a**) homoPBS and (**b**) 2% titanium silicate-1 (TS-1) poly(butylene succinate) (PBS) nanocomposite and shear viscosity changes according to shear rate in (**c**) homoPBS and nanocomposites (TS05: 0.5% TS-1; TS10: 1% TS-1; TS20:2% TS-1).

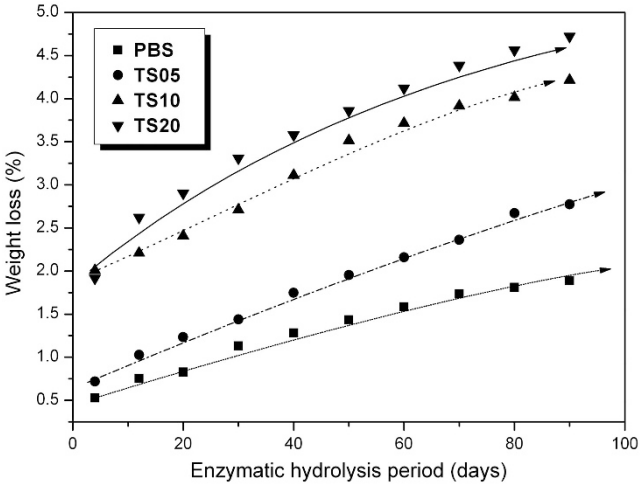

Figure 8 Weight loss versus hydrolysis time for homoPBS and poly(butylene succinate) (PBS)/titanium silicate-1 (TS-1) nanocomposite samples (TS05: 0.5% TS-1; TS10: 1% TS-1; TS20:2% TS-1) during enzymatic hydrolysis at pH 7.4 and 37.5 °C.

that TS-1 zeolite might accelerate the chain orientation of the PBS under shear. When we considered the effect of zeolite content in the nanocomposite on shear viscosity, a 2% nanocomposite showed lower shear viscosity than that of the 0.5% nanocomposite. We explain this reversible result by the presence of zeolitic water released from TS-1 zeolite cages. The TS-1 zeolite absorbed polar molecules, such as water molecules, during the synthetic process and desorbed water molecules in the melt state, resulting in lower dynamic viscosity. The storage moduli of PBS/TS-1 nanocomposites showed higher values than those of homoPBS over the total range of shear rates.

Tensile strength and elongation at break of PBS/TS-1 nanocomposites were increased compared with homoPBS. Improvements of almost 20% for tensile strength and 250% for elongation at break were observed by adding 1% TS-1 zeolite. This reinforcement filler effect of TS-1 zeolite may come from interfacial interaction between the TS-1 zeolite and PBS because of the high surface energy of the zeolite causing the high dispersibility of TS-1 zeolite particles.[53]

We hypothesized that TS-1 zeolite incorporation in PBS could change the surface characteristics and enzymatic hydrolysis of the nanocomposite. Hydrophilicity of the film surface is an important factor for enzymatic hydrolysis. The results of the water contact angle tests indicated that the introduction of TS-1 zeolite can effectively enhance the hydrophilicity of the PBS/TS-1 nanocomposite. After confirming that homoPBS and PBS/TS-1 composite have similar molecular weight by an intrinsic viscosity test, enzymatic hydrolysis testing was conducted and the results are shown in Figure 8. Enzymatic hydrolysis shows saturation in weight loss with the amount and kind of enzyme used. In this work, we observed that TS-1 zeolite acts as an accelerator of enzymatic hydrolysis under 1 wt% content of *Pseudomonas* lipase. As shown in Figure 8, higher zeolite content increased the hydrolysis rate; however, there was no significant difference between the 1 and 2% zeolite content. In the 1 and 2% TS-1 content composite, the quantitative loss of weight of the films was nearly doubled in comparison with those of homoPBS, which indicates that the TS-1 zeolite significantly influenced the enzymatic hydrolysis rate.

Wide-angle X-ray diffraction and SEM images of the surface after enzymatic hydrolysis in both homoPBS and PBS/TS-1 nanocomposite showed no differences between homoPBS and the PBS/TS-1 nanocomposite, except for the clear image of TS-1 zeolite particles on the surface (Figure 9). However, the crystallinity changes in the hydrolyzed sample showed differences in the manner of enzymatic attack on the homoPBS and PBS/TS-1 nanocomposite. There was no change in crystallinity in homoPBS before and after enzymatic hydrolysis. However, in the PBS/TS-1 nanocomposite, the degree of crystallinity, which was similar to that of homoPBS (47%) before hydrolysis, increased to around 52% after hydrolysis. As the surface morphological images in SEM micrographs showed no differences between homoPBS and the PBS/TS-1 nanocomposite, surface erosion alone does not explain the significantly decreased amorphous regions in the PBS/TS-1 nanocomposite. We hypothesize that the TS-1 zeolite can act as a substrate for enzyme loadings, resulting in increased activity in enzymatic degradability for the amorphous phase of the film inside.[54] HomoPBS maintained its intrinsic viscosity (molecular weight) after enzymatic hydrolysis because hydrolysis occurred on the film surface, causing surface erosion. However, the PBS/TS-1 nanocomposite showed significant decreases in intrinsic viscosity after

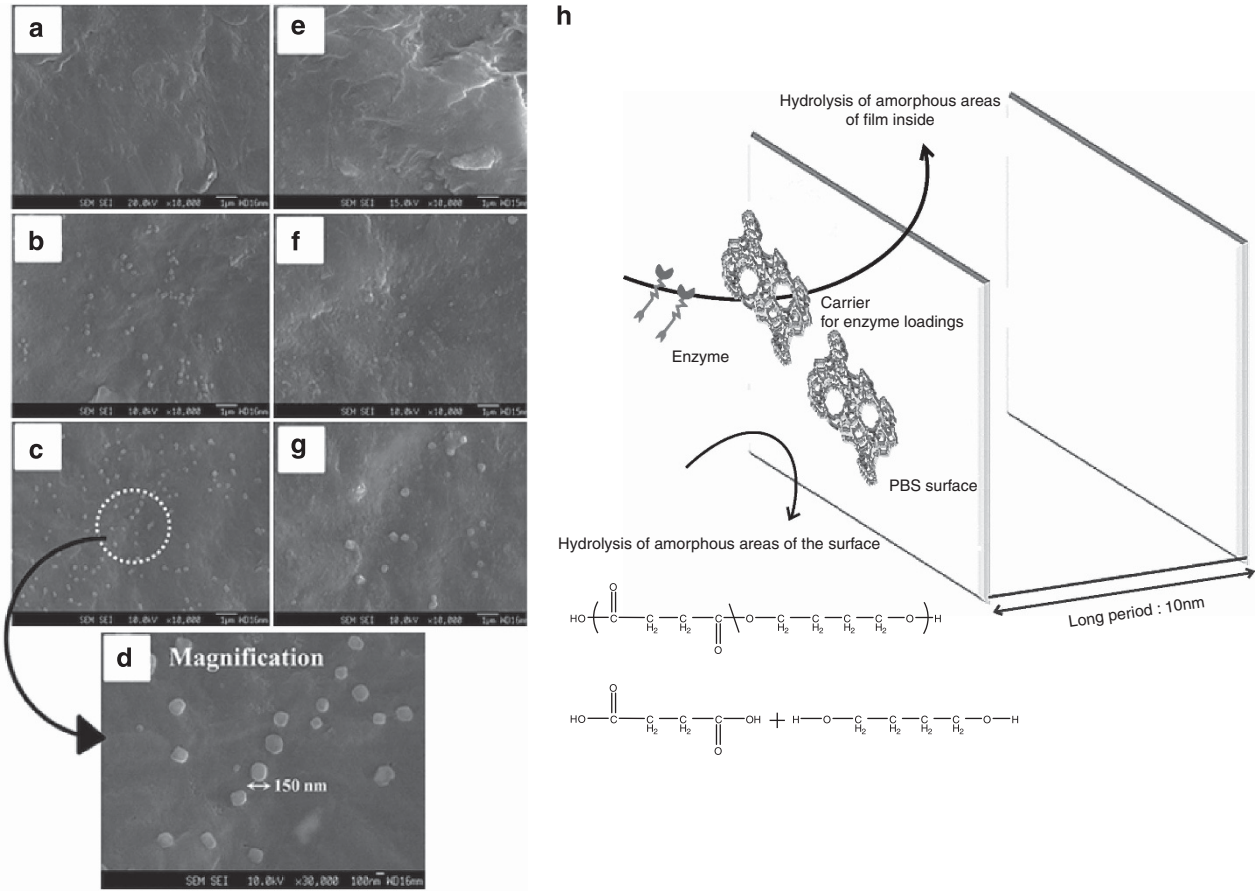

Figure 9 Scanning electron microscopy (SEM) micrographs of surfaces for (**a**) homoPBS, (**b**) 1% titanium silicate-1 (TS-1) composite, (**c**) 2% TS-1 composite, and (**d**) 2% TS-1 composite (magnification) before the enzymatic hydrolysis test and (**e**) homoPBS, (**f**) 1% TS-1 composite, and (**g**) 2% TS-1 composite after the enzymatic hydrolysis test. Schematic representation of enzymatic hydrolysis process for poly(butylene succinate) (PBS)/TS-1 nanocomposite (**h**). A full color version of this figure is available at *Polymer Journal* online.

hydrolysis, indicating that hydrolysis occurred in the amorphous region inside the film, reducing molecular weight.

After considering the results of surface morphology, intrinsic viscosity and crystallinity, we conclude that TS-1 zeolite can be used as a carrier for enzyme loading because of its high desorption capacity and that high enzyme activities significantly affected enzymatic hydrolysis, resulting in a decrease in molecular weight. The typical enzymatic hydrolysis process for PBS/TS-1 nanocomposite is schematically illustrated in Figure 9h.

PBS IONOMER

The synthesis of copolyester based on ionomer

In a previous paper, two types of PBS ionomer (PBSi and POBSi) were polymerized in the presence of dimethyl 5-sulfoisophthalatesodium salt and sodium sulfonate polyethylene glycol (SPEG) via conventional two-step polycondensation.[17,22] Figure 10 shows a representative ^{1}H-nuclear magnetic resonance (NMR) spectrum for homoPBS and POBS-2.0i with characteristic peak assignment to confirm the chemical structure of the POBS ionomer. The chemical structure of PBS can be assigned at 4.1, 2.6 and 1.7 p.p.m., and the integration ratio is 1:1:1, indicating that the synthesis of PBS was completed. Compared with PBS, the peaks of POBS2.0i appear at 3.6 p.p.m., arising from methylene hydrogen at the PEG chain. In addition, methylene hydrogen in SDMF (δ, ε peak) was clearly observed at 6.8 p.p.m. (ε peak). The δ peak did not clearly appear in this sample because of insufficient content. However, the integration ratios of the peaks of α, β, γ and ε, arising from the methylene hydrogens in SPEG, were consistent with the feed composition. This result confirms that SPEG with a sodium sulfonated ionic group was efficiently introduced into the PBS chain.

Table 1 Polymerization data and thermal properties of PBSi and POBSi

Polymer code[a]	*[η] (g·dl^{-1})*[b]	*Reaction time (h)*	T_g[c] *(°C)*	T_m[d] *(°C)*	T_c[d] *(°C)*	$T_m - T_c$ *(°C)*	ΔH_f[d] *(J/g)*
PBS	1.26	6.0	−10.7	114.5	80.1	34.4	79.7
PBSi-1	0.94	6.0	−9.2	113.6	71.2	42.4	77.2
PBSi-2	0.93	6.0	−6.8	112.0	64.8	47.7	73.4
PBSi-3	0.92	7.0	−3.0	110.7	55.8	54.9	63.5
POBS-0.5i	1.00	5.0	−10.5	113.5	68.8	44.7	72.3
POBS-1.0i	1.03	6.0	−9.0	112.8	67.2	45.6	70.1
POBS-2.0i	1.06	6.0	−7.1	110.4	62.6	47.8	64.5

Abbreviations: IV, intrinsic viscosity; PBS, poly(butylene succinate); PBSi and POBSi, two types of PBS ionomer; SPEG, sodium sulfonate polyethylene glycol.
[a]The number at the end of the sample denotes the mole fraction of ionic group. For example, POBS-2.0i represents PBS containing 2.0 mole% of SPEG.
[b]IV was measured by using concentration of 0.2 g dl^{-1} in chloroform at 30 °C.
[c]Measured using dynamic mechanical analysis (DMA), 3 °C min^{-1}.
[d]Measured using differential scanning calorimetry (DSC), 10 °C min^{-1}.

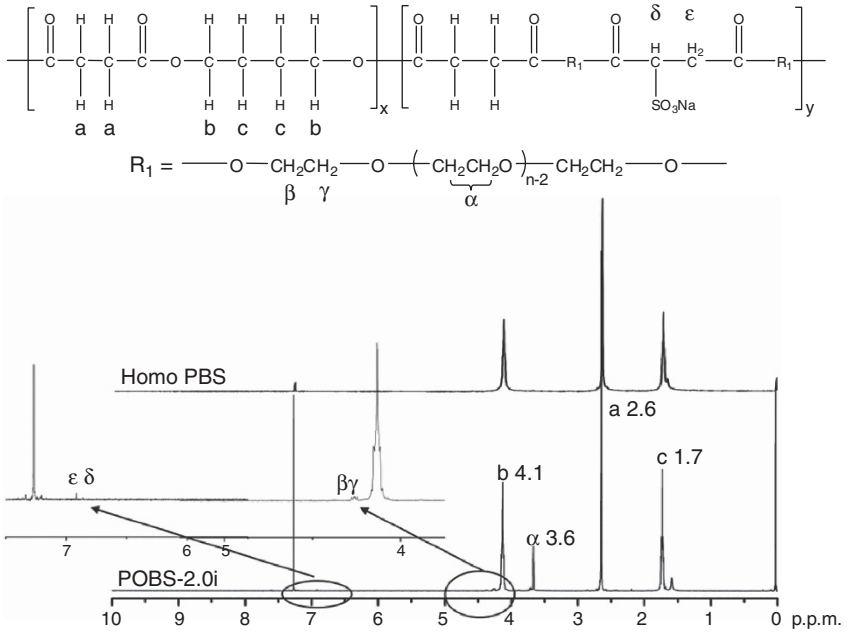

Figure 10 ^{1}H-nuclear magnetic resonance (NMR) spectra of homoPBS and POBS-2.0i in chloroform solution.

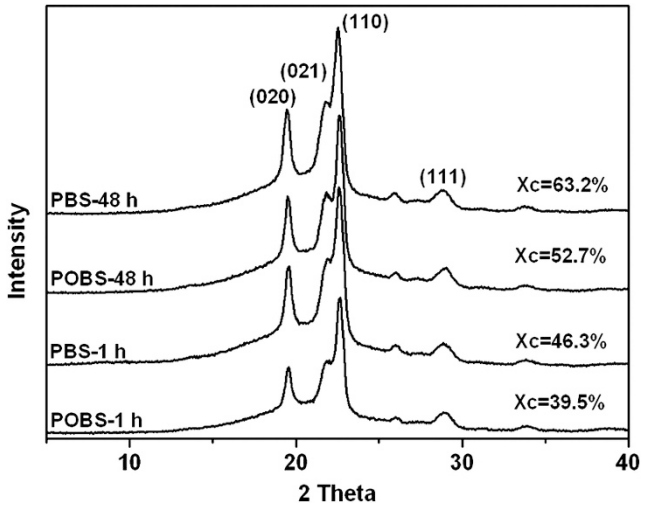

Figure 11 Wide-angle X-ray diffraction (WAXD) pattern and degree of crystallinity of crystallized homoPBS and POBS-2.0i after 1 and 48 h at 80 °C.

Thermal properties and crystallization behavior of PBS ionomer

Random polyester-based ionomers behave like a polymer with high apparent molecular weight because of strong ionic interactions. The characteristics and thermal properties of various PBSi samples are summarized in Table 1. Increasing ion content led to a decrease in the crystallization rate of the POBS ionomer as well as a decrease in the degree of crystallization. In a previous paper,[17] we reported that ionic units might be expelled from the crystalline region, leading to poor packing for the crystallization of the ionomer. Figure 11 shows the WAXD pattern for crystallized PBS and POBS-2.0i samples for 1 and 48 h at 80 °C. When comparing the characteristic peaks of POBS-2.0i with homoPBS, we found that the main peak did not shift at assigned points, indicating that SPEG segments did not affect the crystal lattice. For both 1 and 48 h crystallization times, the diffraction peaks of (020) and (110) for homoPBS were even sharper than those of POBS-2.0i. The variation in the degree of crystallinity between the crystallization times of 1 and 48 h for homoPBS was substantially higher than that of POBS-2.0i. This indicated that the crystal size for POBS-2.0i became imperfect with bulky lateral packing because the ionic groups in SPEG segments led to expulsion from the crystalline region, with the result that POBS-2.0i showed a low degree of packing perfection irrespective of crystallization time compared with homoPBS.[18,37]

In a previous study of PBSi,[18] we investigated the spherulitic morphology of PBSi at the initial step in the crystallization process using transmission electron microscopy, as shown in Figure 12. The spherulites of homoPBS displayed a well-defined fibrillar pattern (Figure 12a). In contrast, the spherulites of PBSi-3 showed an irregular ringed pattern without a distinct spherulite center (Figure 12b). As shown in Figure 12c, transmission electron microscopy images of PBSi-3 exhibited a petal-like structure with branching of the subsidiary lamellae radiating from the center. Ionic clusters expelled from the crystalline lamellae were also observed, appearing as aggregation clusters with sizes between 40 and 50 nm. These are characteristic morphologies of PBSi, assuming that the clusters impede the regular lamellae growth of an axialite-type. For semi-crystalline ionomers, considering the fact that ionic domains segregate into regions outside the lamellar stacks and restrict chain mobility, we hypothesize that the chains restricted by ionic aggregates have difficulty folding into crystalline lamellae.

Physical properties of ionomers

Figures 13a and b show the storage moduli (G') and tan δ of PBSi ionomer samples plotted against temperature. PBSi-3 showed the highest storage modulus up to the rubbery plateau region, probably due to the strong physical cross-linkage by electrostatic attractive forces between ionic groups. On the other hand, the storage modulus for PBSi-5 dropped rapidly above the glass transition region with increasing temperature, which may have been due to the reverse effect

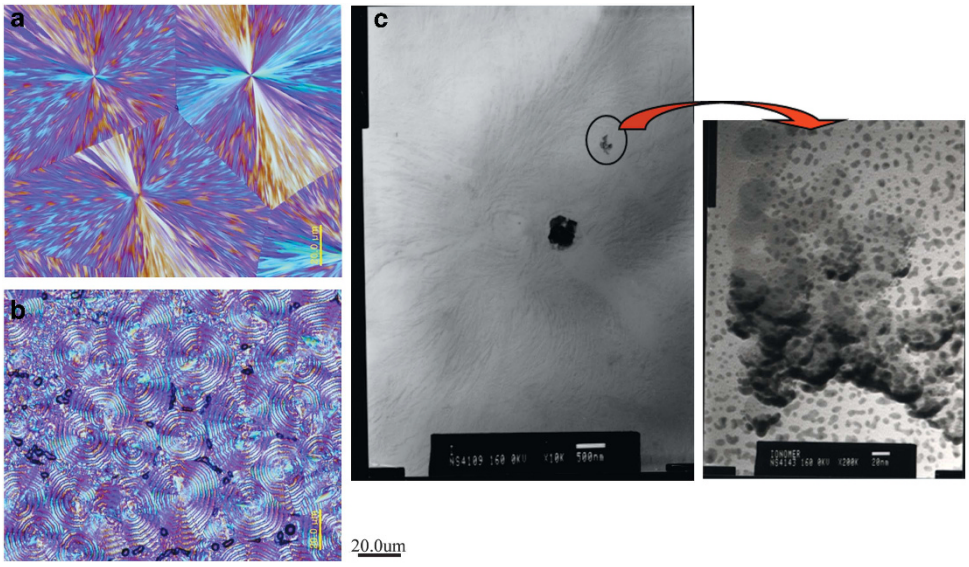

Figure 12 POM morphologies of samples crystallized at wide-angle X-ray diffraction (WAXD) pattern and 80 °C: (**a**) homoPBS, (**b**) PBSi-3 and transmission electron microscopy (TEM) images of PBSi-3 (**c**).

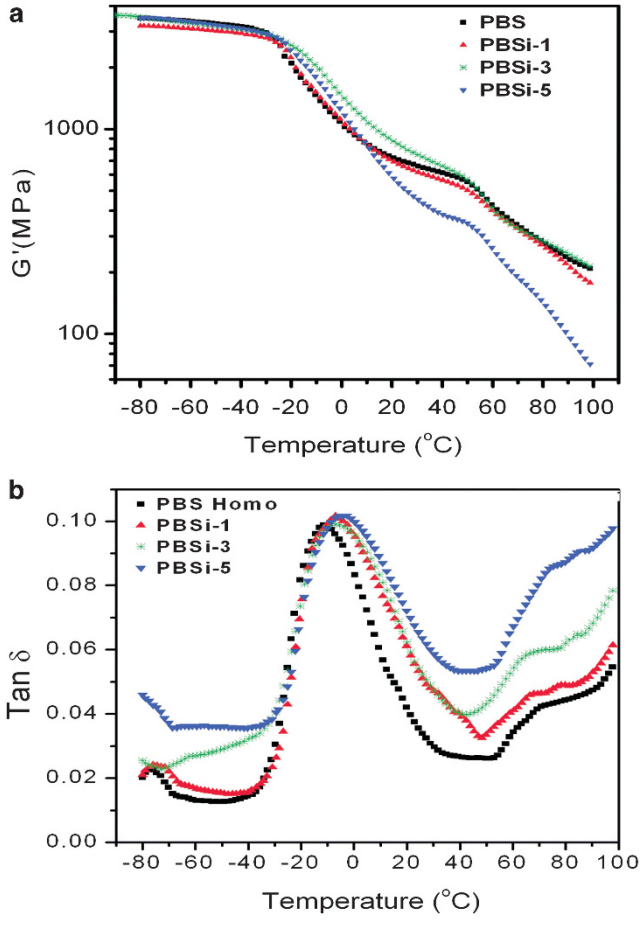

Figure 13 Poly(butylene succinate) (PBS) ionomer of (**a**) storage modulus and (**b**) tan δ ranged from −80 to 100 °C.

of physical cross-linking, resulting from preferential intramolecular ion-pair associations. Intramolecular ion-pair associations lead to the collapse of the polymer chain, which may reduce both the radius of gyration and the viscosity.[55] The tan δ curves for PBS ionomer samples showed two T_g's, as shown in Figure 13b. The main peak was assigned as the T_g of the matrix, whereas the shoulder at higher temperature reflected the T_g corresponding to the ion cluster region.

To investigate the rheological behavior of the ionomer, we performed measurements using a dynamic oscillatory viscometer (ARES, Rheometric Scientific, Piscataway, NJ, USA) with parallel plate geometry, 20 mm diameter and 1.0 mm gap distance between the parallel plates on POBS ionomer samples. The experiment was performed with a frequency sweep that ranged from 0.1 to 500 rad s^{-1} at a 10% strain level at 150 °C.

The initial melt viscosities of all POBS ionomers at low frequency (Figure 14a) were higher than that of homoPBS. This indicates that the strong physical interactions between ionic groups have decisive effects on melt viscosity. The melt viscosity of ionomers is determined by the intrinsic molecular weight of the polymer and the extent of physical linkages because of ionic aggregates.[16,19] POBS-0.5i has the highest melt viscosity among the examined ionomers, and the degree of shear thinning showed a uniform slope, similar to that seen in the homoPBS in all tested ranges (Figure 14a). The viscosities of POBS-1.0i and 2.0i are lower than that of POBS-0.5i at low shear and drop rapidly at about 10^1 ω rad s^{-1} with increasing shear force due to ionic interactions that are mainly dominated by intermolecular ionic associations below a critical ionic content, whereas intramolecular associations also increased with increasing ionic content and caused reductions in both the radius of gyration and the viscosity. POBS-0.5i may be influenced by intermolecular ion pair associations, leading to higher viscosity than that of PBS at high frequency. However, in the case of POBS-1.0i and 2.0i, intramolecular ionic associations can accelerate PBS molecular chain orientation under high shear rates. These results suggest that strong physical linkages among ionic

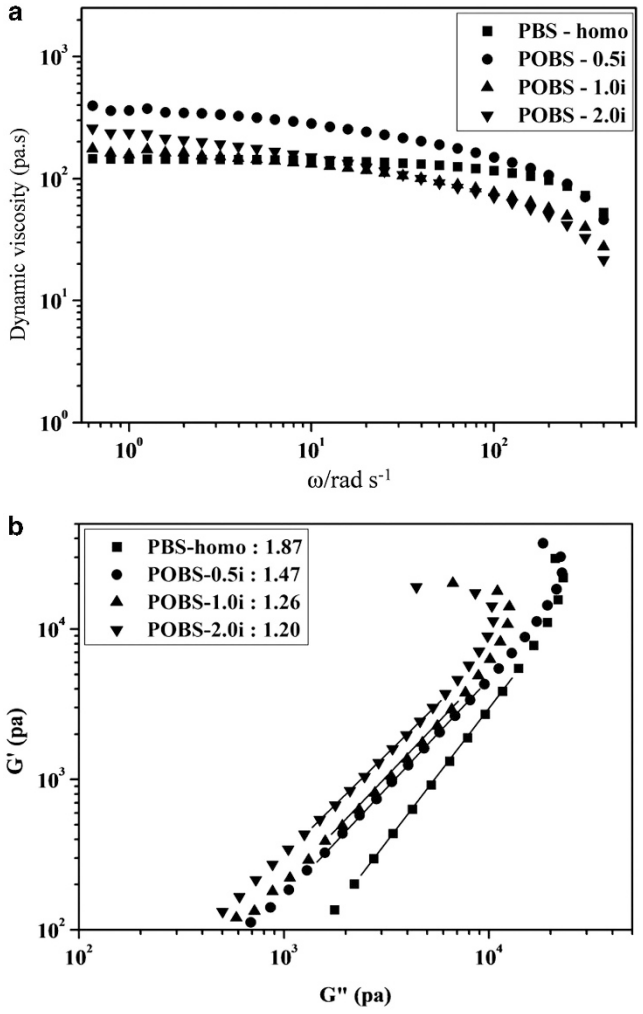

Figure 14 Rheological properties of (**a**) melt viscosity and (**b**) Cole–Cole plots for homoPBS and POBS ionomers at 150 °C.

groups affect melt rheological properties and structure because of the collapse of ionic aggregates with increased shear force. A Cole–Cole plot of PBS and POBS ionomers is shown in Figure 14b. The slope of the POBS ionomers became gradually lower with increasing SPEG content.

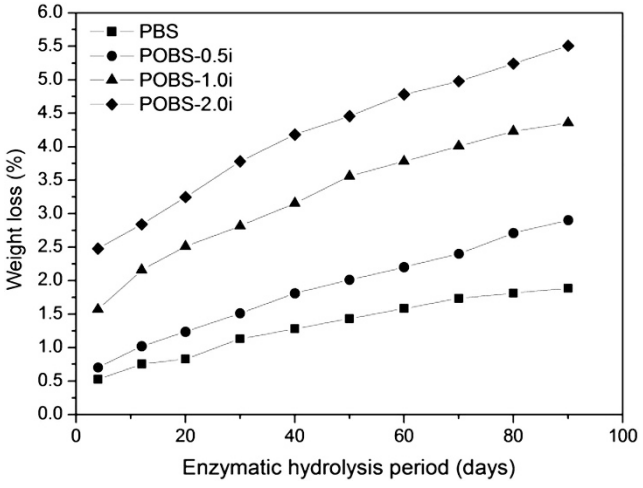

Figure 15 Weight loss versus hydrolysis time for homoPBS and POBS ionomer during enzymatic hydrolysis at pH 7.4 and 37.5 °C.

Table 2 Changes in crystallinity for homoPBS and POBS-2.0i

Sample	*Crystallinity*
PBS (1 h)	46.3
POBS—2.0i (1 h)	39.5
PBS (48 h)	63.2
POBS—2.0i (48 h)	52.7

Abbreviation: PBS, poly(butylene succinate).

Enzymatic hydrolysis of copolyester-based ionomers

The degree of enzymatic hydrolysis was estimated based on the loss of weight per initial weight during the enzymatic hydrolysis test, as shown in Figure 15. The films were prepared by compression molding with a thickness of 0.3 mm. Several factors must be considered to identify the cause of increased enzymatic hydrolysis. The degree of enzymatic hydrolysis depends on the degree of crystallinity, chemical structure and the hydrophilic/hydrophobic balance in the polymer matrix.[2,56] Therefore, we investigated several factors related to enzymatic hydrolysis. The weight loss of enzymatic hydrolysis was accelerated with increasing ionic content in comparison with homoPBS. The enhanced hydrophilicity of POBS ionomer films made the surface more vulnerable to hydrolysis. The hydrophilicity of the surfaces of biodegradable polymers is a decisive factor in biodegradation rates because the water absorbed on the polymer surface leads to enhanced enzymatic hydrolysis behavior.[2] The variation in the degree of crystallinity between crystallization times of 1 and 48 h for homoPBS was substantially higher than that of POBS-2.0i. This indicated that the crystal size for POBS-2.0i became imperfect with bulky lateral packing because the ionic groups in SPEG segments lead to expulsion from the crystalline region, with the result that POBS-2.0i showed a low degree of packing perfection irrespective of crystallization time compared with homoPBS, as shown in Table 2. Consequently, rapid enzymatic hydrolysis of POBS is a reasonable conclusion given that the increased amorphous regions are largely responsible for higher enzymatic hydrolysis rates.

CONCLUSION

We reviewed PBS-related research on the synthesis of copolyester based on ionomers, the preparation of composites with various inorganic fillers focused on the enhanced physical properties and enzymatic hydrolysis behavior to expand the potential application fields of this biodegradable polymer. We used two inorganic materials to investigate how nanoparticles could be dispersed in a PBS matrix and to identify the properties that could be advanced by making well dispersed PBS nanocomposites. We introduced a urethane group on the clay surface to develop physically enhanced PBS/MMT nanocomposites. We studied the characteristics of biodegradable copolyester-based ionomers. PBS ionomers showed improved mechanical physical properties because of ionic interactions. The enzymatic hydrolysis behavior of PBS ionomers was drastically accelerated with increasing ionic content because of reduction in crystallinity and improved hydrophilicity.

1 Nagata, M., Machida, T., Sakai, W. & Tsutsumi, N. Synthesis, characterization, and enzymatic degradation studies on novel network aliphatic polyesters. *Macromolecules* **31,** 6450–6454 (1998).
2 Tsuji, H. & Miyauchi, S. Enzymatic hydrolysis of poly(lactide)s: effects of molecular weight, L-lactide content, and enantiomeric and diastereoisomeric polymer blending. *Biomacromolecules* **2,** 597–604 (2001).
3 Gau, Z., Abe, H., Kurokawa, H. & Doi, Y. Solid-state microstructures, thermal properties, and crystallization of biodegradable poly(butylene succinate) (PBS) and its copolyesters. *Biomacromolecules* **2,** 605–613 (2001).
4 Yoshie, N., Oike, Y., Kasuya, K., Doi, Y. & Inoue, Y. Change of surface structure of poly(3-hydroxybutyrate) film upon enzymatic hydrolysis by PHB depolymerase. *Biomacromolecules* **3,** 1320–1326 (2002).
5 Kobori, Y., Iwata, T., Doi, Y. & Abe, H. Synthesis, solid-state structure, and surface properties of end-capped poly(L-lactide). *Biomacromolecules* **5,** 530–536 (2004).
6 Yu, X., Feng, J. & Zhuo, R. Preparation of hyperbranched aliphatic polyester derived from functionalized 1,4-dioxan-2-one. *Macromolecules* **38,** 6244–6247 (2005).
7 Kim, E. J., Uyama, H., Doi, Y., Ha, C. S. & Iwata, T. Crystal structure and morphology of poly(12-dodecalactone). *Biomacromolecules* **6,** 572–579 (2005).
8 Kurokawa, K., Yamashita, K., Doi, Y. & Abe, H. Structural effects of terminal groups on nonenzymatic and enzymatic degradations of end-capped poly(L-lactide). *Biomacromolecules* **9,** 1071–1078 (2008).
9 Ihn, K. J. & Yoo, E. S. Structure and morphology of poly(tetramethylene succinate) crystals. *Macromolecules* **28,** 2460–2464 (1995).
10 Ray, S. S., Okamoto, K. & Okamoto, M. Structure−property relationship in biodegradable poly(butylene succinate)/layered silicate nanocomposites. *Macromolecules* **36,** 2355–2367 (2003).
11 Okamoto, K., Ray, S. S. & Okamoto, M. J. New poly(butylene succinate)/layered silicate nanocomposites. II. Effect of organically modified layered silicates on structure, properties, melt rheology, and biodegradability. *Polym. Sci. Part B: Polym. Phys.* **41,** 3160–3172 (2003).
12 Park, J. W., Kim, D. K. & Im, S. S. Biodegradable polymer blends of poly(L-lactic acid) and gelatinized starch. *Polym. Int* **51,** 239–244 (2002).
13 Abe, H., Doi, Y. & Hagiwara, T. Physical properties and enzymatic degradability of copolymers of (R)-3-hydroxybutyric acid and (S,S)-lactide. *Polymer (Guildf.)* **39,** 59–674 (1998).
14 Lim, J. S., Lee, Y. G. & Im, S. S. Influence of ionic association on the nonisothermal crystallization kinetics of sodium sulfonate poly(butylene succinate) ionomer. *J. Polym. Sci: Part B: Polym. Phys* **46,** 925–937 (2008).
15 Howard, S. J. & Knutton, S. Isomorphism in aliphatic copolyesters. *Polymer (Guildf)* **9,** 527–534 (1968).
16 Han, S. I., Yoo, Y. T., Kim, D. K. & Im, S. S. Crystallization behavior of degradable poly(butylene succinate) ionomers and their biocompatibility. *Macromol. Biosci.* **4,** 199–207 (2004).
17 Han, S. I., Im, S. S. & Kim, D. K. Dynamic mechanical and melt rheological properties of sulfonated poly(butylene succinate) ionomers. *Polymer (Guildf.)* **44,** 7165–7173 (2003).
18 Han, S. I., Lee, W. D., Kim, D. K. & Im, S. S. Morphology and crystallization behavior of poly(butylene succinate)-based ionomers (PBSi). *Macomol. Rapid Commun.* **25,** 753–758 (2004).
19 Ishida, K., Han, S. I., Inoue, Y. & Im Novel, S. S. Poly(butylene succinate)-based ionomers with sulfonated succinate units: synthesis, morphology, and the unique nucleation effect on crystallization. *Macromol. Chem. Phys.* **206,** 1028–1034 (2005).
20 Ishida, K., Han, S. I., Im, S. S. & Inoue, Y. Effects of fusion temperature and metal ion variation on crystallization of lightly ionized poly(butylene succinate). *Macromol. Chem. Phys.* **208,** 146–154 (2007).
21 Han, S. I., Kim, B. S., Kang, S. W., Shirai, H. & Im, S. S. Cellular interactions and degradation of aliphatic poly(ester amide)s derived from glycine and/or 4-amino butyric acid. *Biomaterial* **24,** 3453–3462 (2003).
22 Hwang, S. Y., Jin, X. Y., Yoo, E. S. & Im, S. S. Synthesis, physical properties and enzymatic degradation of poly (oxyethylene-b-butylene succinate) ionomers. *Polymer (Guildf.)* **52,** 2784–2791 (2011).
23 Nguyen, D., Kim, J. S., Guiver, M. D. & Eisenberg, A. J. Clustering in carboxylated polysulfone ionomers: a characterization by dynamic mechanical and small-angle X-ray scattering methods. *Polym. Sci. Part B: Polym. Phys.* **37,** 3226–3232 (1999).
24 Weiss, R. A. & Yu, W. C. Viscoelastic behavior of very lightly sulfonated polystyrene ionomers. *Macromolecules* **44,** 7165–7173 (2003).
25 Kim, J. S., Hong, M. C. & Nah, Y. H. Effects of two ionic groups in an ionic repeat unit on the properties of styrene ionomers. *Macromolecules* **35,** 155–160 (2002).
26 Gan, Z., Abe, H. & Doi, Y. Crystallization, melting, and enzymatic degradation of biodegradable poly(butylene succinate-co-14 mol % ethylene succinate) copolyester. *Biomacromolecules* **2,** 313–321 (2001).
27 Kuwabara, K., Gan, Z., Nakamura, T., Abe, H. & Doi, Y. Molecular mobility and phase structure of biodegradable poly(butylene succinate) and poly(butylene succinate-co-butylene adipate). *Biomacromolecules* **3,** 1095–1100 (2002).
28 Rizzarelli, P., Impallomeni, G. & Montaudo, G. Evidence for selective hydrolysis of aliphatic copolyesters induced by lipase catalysis. *Biomacromolecules* **5,** 433–444 (2004).
29 Yang, J., Tian, W., Li, Q., Li, Y. & Cao, A. Novel biodegradable aliphatic poly(butylene succinate-co-cyclic carbonate)s bearing functionalizable carbonate building blocks: II. Enzymatic biodegradation and in vitro biocompatibility assay. *Biomacromolecules* **5,** 2258–2268 (2004).
30 Papageorgiou George, Z. & Bikiaris Dimitrios, N. Synthesis, cocrystallization, and enzymatic degradation of novel poly(butylene-co-propylene succinate) copolymers. *Biomacromolecules* **8,** 2437–2449 (2007).
31 Li, Y. D., Zeng, J. B., Wang, X. L., Yang, K. K. & Wang, Y. Z. Structure and properties of soy protein/poly(butylene succinate) blends with improved compatibility. *Biomacromolecules* **9,** 3157–3164 (2008).
32 Tserki, V., Matzinos, P., Pavlidou, E., Vachliotis, D. & Panayiotou, C. Biodegradable aliphatic polyesters. Part I. Properties and biodegradation of poly(butylene succinate-co-butylene adipate). *Polym. Degrad. Stab.* **91,** 367–376 (2006).
33 Cao, A., Okamura, T., Ishiguro, C., Nakayama, K., Inoue, Y. & Masuda, T. Studies on syntheses and physical characterization of biodegradable aliphatic poly(butylene succinate-co-epsilon-caprolactone)s. *Polymer (Guildf.)* **43,** 671–679 (2002).
34 Park, S. J., Lee, Y. M. & Hong, S. K. Release behaviors of porous poly(butylene succinate)/poly(epsilon-caprolactone) microcapsules containing indomethacin. *Colloid Surf. B* **47,** 211–215 (2006).
35 Park, S. B., Hwang, S. Y., Moon, C. H., Im, S. S. & Yoo, E. S. Plasticizer effect of novel PBS ionomer in PLA/PBS ionomer blends. *Macromol. Res.* **18,** 463–471 (2010).
36 Ishida, K., Han, S. I., Im, S. S. & Inoue, Y. Effects of fusion temperature and metal ion variation on crystallization of lightly ionized poly(butylene succinate). *Macromol. Chem. Phys* **208,** 146–154 (2007).
37 Han, S. I., Kang, S. W., Kim, B. S. & Im, S. S. A novel polymeric ionomer as a potential biomaterial: crystallization behavior, degradation, and in-vitro cellular interactions. *Adv. Funct. Mater.* **15,** 367–374 (2005).
38 Hwang, S. Y., Yoo, E. S. & Im, S. S. Effect of the urethane group on treated clay surfaces for high-performance poly(butylene succinate)/montmorillonite nanocomposites. *Polym. Degrad. Stab.* **94,** 2163–2169 (2009).
39 Han, S. I., Lim, J. S., Kim, D. K., Kim, M. N. & Im, S. S. In situ polymerized poly(butylene succinate)/silica nanocomposites: physical properties and biodegradation. *Polym. Degrad. Stab.* **93,** 889–895 (2008).
40 Fornes, T. D., Hunter, D. L. & Paul, D. R. Nylon-6 nanocomposites from alkylammonium-modified clay: the role of alkyl tails on exfoliation. *Macromolecules* **37,** 1793–1798 (2004).
41 Rong, M. Z., Zhang, M. Q., Zheng, Y. X., Zeng, H. M., Walter, R. & Friedrich, K. Structure-property relationships of irradiation grafted nano-inorganic particle filled polypropylene composites. *Polymer (Guildf.)* **42,** 167–183 (2001).
42 Wu, T. M. & Liu, C. Y. Poly(ethylene 2,6-naphthalate)/layered silicate nanocomposites: fabrication, crystallization behavior and properties. *Polymer (Guildf.)* **46,** 5621–5629 (2005).
43 Maio, E. D., Lannace, S., Sorrentino, L. & Nicolais, L. Isothermal crystallization in PCL/clay nanocomposites investigated with thermal and rheometric methods. *Polymer (Guildf.)* **45,** 8893–8900 (2004).
44 van Bekkum, H., Flanigen, E. M. & Jansen, J. C. (eds). *Introduction to Zeolite Science and Practice* (Elsevier, Amsterdam, 1991).
45 Pérez-Ramírez, J., Verboekend, D., Bonilla, A. & Abelló, S. Zeolite catalysts with tunable hierarchy factor by pore-growth moderators. *Adv. Funct. Mater.* **19,** 3972–3979 (2009).
46 Srivastava, R., Choi, M. K. & Ryoo, R. Mesoporous materials with zeolite framework: remarkable effect of the hierarchical structure for retardation of catalyst deactivation. *Chem. Commun* **43,** 4489–4491 (2006).
47 Kortunov, P., Vasenkow, S., Chmelik, C., Kärger, J., Ruthven, D. M. & Wloch, J. Influence of defects on the external crystal surface on molecular uptake into MFI-type zeolites. *Chem. Mater.* **16,** 3552–3558 (2004).
48 Pan, D. H., Yuan, P., Zhao, L. Z., Liu, N., Zhou, L., Wei, G. F., Zhang, J., Ling, Y., Fan, Y., Wei, B. Y., Liu, H. Y., Yu, C. Z. & Bao, X. New understanding and simple approach to synthesize highly hydrothermally stable and ordered mesoporous materials. *Chem. Mater.* **21,** 5413–5425 (2009).
49 Lee, Y. J., Kim, S. J., Ahn, D. C. & Shin, N. S. Confined water clusters in a synthetic rubidium gallosilicate with zeolite LTL topology. *Chem. Mater.* **19,** 2277–2282 (2007).
50 Grieneisen, J. L., Kessler, H., Fache, E. & Le Govic, A. M. Synthesis of TS-1 in fluoride medium. A new way to a cheap and efficient catalyst for phenol hydroxylation. *Micropor. Mesopor. Mater.* **37,** 379–386 (2000).
51 Phonthammachai, N., Krissanasaeranee, E., Gulari, E., Jamieson, A. M. & Wongkasemjit, S. Crystallization and catalytic activity of high titanium loaded TS-1 zeolite. *Mater. Chem. Phys.* **97,** 458–467 (2006).
52 Li, Y. G., Lee, Y. M. & Porter, J. F. J. The synthesis and characterization of titanium silicalite-1. *Mater. Sci.* **37,** 1959–1965 (2002).
53 Frisch, H. L. & Mark, J. E. Nanocomposites prepared by threading polymer chains through zeolites, mesoporous silica, or silica nanotubes. *Chem. Mater* **8,** 1735–1738 (1996).
54 Wang, Y. & Caruso, F. Macroporous zeolitic membrane bioreactors. *Adv. Funct. Mater.* **14,** 1012–1018 (2004).
55 Lundberg, R. D. & Phillips, R. R. Solution behavior of metal sulfonate ionomers. 2. effects of solvents,. *J. Polym. Sci. Pol. Phys.* **20,** 1143 (1982).
56 Hwang, S. Y., Yoo, E. S. & Im, S. S. Effects of TS-1 zeolite structures on physical properties and enzymatic degradation of poly (butylene succinate) (PBS)/TS-1 zeolite hybrid composites. *Polymer (Guildf.)* **52,** 965–975 (2011).

Sung Y Hwang works as a senior research engineer at SKC Advanced Technology R&D Center. He received his Master Degree (2008) and PhD (2011) in fiber and polymer engineering at Hanyang University. His main research is related to the area of biodegradable polymer, polymeric biomaterials such as drug delivery system, nanocomposites, polymer crystallization and morphology.

Eui S Yoo works as principal researcher at the Department of Textile Convergence of Biotechnology and Nanotechnology, Korea Institute of Industrial Technology. He received his Master Degree (1993) and PhD (1998) in fiber and polymer engineering at Hanyang University. He worked as postdoc of Department of Polymer Science and Engineering at the University of Massachusetts, Amherst, MA, USA from 2001 to 2004. His main research interests include the hetero cyclic high-performance polymer, environmental degradation polymer, polymer crystallization and morphology, color filter for LCD display, and dyestuff.

Seung S Im works as a professor at the Department of Fiber and Polymer Engineering at Hanyang University. He graduated from the Department of Textile Engineering at Hanyang University and received his Master Degree (1975) and PhD (1978) in organic material at Tokyo Institute of Technology, Japan. He was a president of Korean Fiber Society at 2003 and Dean of Graduate School of Engineering, Hanyang University from 2008 to 2010. He received 'International Award of Polymer' at the Society of Polymer Science, Japan. His group's current interests include biodegradable polyester, polymeric biomaterial, nanocomposites, conductive polymer and dye-sensitized solar cells. He has published >140 papers in several international journals.